

DROP SIZE EFFECTS IN SPRAY DETONATIONS

by

E.K. Dabora, K.W. Ragland, and J.A. Nicholls

Gas Dynamics Laboratories

Department of Aerospace Engineering

The University of Michigan, Ann Arbor, Michigan 48105

NASA-54(07)

SUMMARY

Recent experimental results on the development and propagation of detonations in sprays of liquid diethylcyclohexane (DECH) in gaseous oxygen are presented. Three drop sizes are used: 290μ , 940μ and 2600μ . It is found that the smaller the drop size, the faster the detonation develops into a steady state. The steady velocity for mixtures ranging from 0.2-1.0 in equivalence ratio, is found to be lower than the ideal Chapman-Jouguet velocity. The difference is 2-10% for the 290μ and the 940μ sprays and 30-35% for the 2600μ . Heat transfer measurements and inferred frictional losses to the walls are used, in conjunction with a reaction length assumed to be controlled by the break-up of the drops, to arrive at a relationship between the experimental and the ideal (no loss) velocities. The relationship shows direct dependence of velocity difference on drop size and results in a calculated difference of 4%, 10%, and 26% for the 290μ , 940μ and 2600μ sprays respectively.

H.C. —
M.F. —

FACILITY FORM 602	<i>N68 33512</i>	(THRU)
	(ACCESSION NUMBER)	
	<i>28</i>	
	(PAGES)	
	<i>CR-96366</i>	
	(NASA CR OR TMX OR AD NUMBER)	
		<i>33</i>
		(CATEGORY)

Schlieren and direct light photographs of the phenomenon are also presented. They show a rather complicated structure of the flow field behind the front due to the interaction of the gaseous convective flow and the initially stationary drops.

INTRODUCTION

The effects of drop size on the propagation of detonations in a heterogeneous mixture (a liquid fuel spray in gaseous oxygen) which will be presented in this paper represent a part of a continuing effort on which we have previously reported in the literature¹. Spray detonations have been treated both theoretically and experimentally in the past, but the effects of an experimental systematic variation of mixture ratio and drop size have not been evaluated. In the theoretical treatment of Williams², it was concluded that two phase detonations would be impossible because of the extended reaction zone arising from the slow evaporation process. However, his conclusion was tempered by two observations: first, that sprays below 10μ drop diameter would behave like a gaseous mixture and second, that drop shattering might circumvent the slow evaporation and thus support detonation. Indeed our findings¹ have shown that drop shattering does play an important role.

Webber³ and Cramer⁴ were the first to perform spray detonation experiments by using a combustion driven shock tube to generate a

shock which initiated a detonation in the spray. However, their emphasis was on the development stages of the phenomenon. Furthermore, due to their method of spray formation, accurate knowledge of the mixture ratio was not possible. This remark also applies to the work of Morris et al⁵ on the development of detonations in a mixture of kerosene and oxygen.

The main objective of this paper is to present the observed effect of drop size on the development time of the detonation, and the effect of both mixture ratio and drop size on the steady propagation velocity. In particular the latter will be shown to be lower than the ideal Chapman-Jouguet (CJ) velocity and that the difference is explainable by the long reaction zone, which is controlled by the drop breakup time, and the consequent high frictional and heat losses to the tube walls.

EXPERIMENTAL APPARATUS

The experimental facility for studying spray detonations consists of the following main items: (a) a device for producing a fuel spray, (b) a tube in which the spray is evenly distributed with the gaseous oxygen, (c) an initiation device, and (d) instrumentation for the operation of the facility and for data acquisition. Figure 1 shows a

schematic diagram of the setup used for the experiments reported here. The detonation tube is a square tube $12 \frac{1}{3}$ ft long with an internal side of 1.64 in. It is provided with two viewing sections. The top section is used for observation of the spray before a run is made to insure that the spray is properly set up. The driven section of the initiating tube is flush mounted at a 45° angle to one side wall of this observation section. The lower viewing section has an 11 in. long window with its center located at 83 in. from the top of the tube and is used for photographic observations during a run. Mounted flush with the inside wall of the tube, are pressure switches which, in conjunction with a multiple RC circuit and an oscilloscope operated in a raster mode, are used for velocity measurement. Pressure and heat transfer measurements are made with piezoelectric pressure transducers⁶ and thin film heat transfer gauges. These transducers are located in general at stations near the test section where steady or nearly steady conditions prevail.

The device for producing monodisperse sprays is designed according to the guidelines set forth by Dabora⁷. It consists of a small cylindrical chamber fitted at its bottom with a plate having several capillary needles in parallel. The fuel capillary jets issuing from the needles are broken up into regular size drops when the top base of the chamber which is made of a brass shim stock is vibrated at a frequency compatible with the jet velocity⁷.

The operational procedure can be followed by referring to Fig. 1. The fuel flow through the drop generator and the signal generator frequency and amplitude are set and the drops are checked to insure that regular sizes are produced. Then the solenoid valve is closed, the detonation tube is dried with air, and then purged and filled with oxygen at atmospheric pressure. The initiating tube is evacuated and filled with $2\text{H}_2 + \text{O}_2$ mixture, usually at atmospheric pressure. Then a cycle of events leading to detonation is started with the micro-switch timer which has a total cycle time of 10 sec with circuit controls adjustable to any fraction of the cycle to within 0.25 sec resolution. These events are as follows:

1. The solenoid valve is opened so that the fuel flows through the drop generator for a preset length of time controlled by the timer. The duration is sufficient to allow the first drops to reach the bottom of the tube and is usually 2-4 sec. The flow is terminated .25 sec after the detonation spark plug is fired.
2. The mechanical shutter is then opened.
3. A spark-source (.2 μ sec duration) or a flash unit (1 msec duration) are fired so that either photographs of the spray before detonation or of the detonation itself are obtained.

When necessary, the light source is controlled by the event itself as shown by the dotted path in Fig. 1. We have also

used an electromagnetic shutter⁸ (not shown) which is also controlled by the event. It has an exposure time of about 200-300 μ sec and is placed at the focal point of the second schlieren lens. It is timed to be open when the spark light source is on and its main purpose, therefore, is to limit the direct light from the burning mixture behind the detonation front.

4. Finally, the spark plug for starting the gaseous detonation in the initiation tube is energized. This detonation produces a shock wave in the driven section which hits the spray and thus initiates a detonation in the main tube.

EXPERIMENTAL OBSERVATIONS

A. Photographic

Three drop sizes were used in our experiments, namely 290 μ , 940 μ , and 2600 μ and the fuel was diethylcyclohexane (DECH). As was mentioned in the preceding section, a picture of the spray in the test section is usually taken shortly before the detonation wave passes over it. The purpose, is to allow an accurate measurement of the mixture ratio. For the smaller drops where coalescence of the drops takes place as they fall along the tube and where some of the drops are lost by adherence to the tube walls, the photograph provides the only means of calculating the mixture ratio. Figure 2a shows a photograph of the 290 μ spray where some large drops due to coalescence

can be seen. Similarly, Fig. 2b shows the 940 μ spray where somewhat less coalescence has taken place. It is clear, however that a reasonably accurate mixture ratio can be obtained from such photographs. On the other hand, for a single stream of 2600 μ drops as shown in Fig. 2c, no coalescence can be seen. For such a stream, it is, of course, possible to calculate the mixture ratio from a knowledge of the volumetric flow rate and the shedding frequency, which is the same as the vibration frequency imposed on the drop generator.

Examples of streak photographs of the detonation phenomenon are shown in Fig. 3-5. Figure 3 is a schlieren of a detonation in 290 μ spray. (All streak photographs are shown in a somewhat unconventional manner, in that distance increases vertically downward to correspond to the physical situation, i. e. a wave travelling downward.) The dark horizontal lines before the detonation front represent drops which happen to be in the slit and the dark zone behind the front shows the extent of the interaction between the gaseous convective flow and the drops. This zone, which is interpreted to represent the breakup time of the drop, is estimated in this example to be about 20 μ sec for a detonation travelling at 5500 ft/sec. The equivalence ratio in this case is 0.3.

Figure 4 is a combination shadow and direct light streak photograph for a 940 μ spray. The schlieren part is the bright central portion which is 5 in. wide. The traces of some drops are apparent and it is evident that some combustion takes place before complete breakup. More details of the trajectory of the drops and their fate

can be obtained from photographs of the detonation of a single stream of 2600μ drops as shown in Fig. 5 which is again a combined shadow and direct light photograph. As the drop is passed by the front shock wave, it starts to deform instantly as can be seen from the shadow portion of the photograph. Because the convective gas flow is supersonic, a bow shock appears with its standoff distance increasing as the drop continues to deform. A wake behind the drop, evidently composed of small particles of fuel stripped away by the convective flow and mixed with the gaseous oxygen, starts to ignite violently and apparently obliterates the bow shock of the preceding drop. Some secondary shocks arising from the explosion of the wake can be seen in the shadow portion of the photograph. In some cases it was found that combustion started at the stagnation point of the drop.

Further details of the process taking place in the tube as a whole can be obtained from spark schlieren photographs such as shown in Fig. 6. In this figure, which is a composite of three photographs taken at three different time delays and arranged so as to show details for about 12 in. behind the front, one can see the deformation of the drop, the wake, the bow shock and the spherical explosion wave around the second drop behind the front. Pressure measurements confirmed the existence of the spherical explosion in that spikes of double-to triple the pressure behind the front were observed. One can also see wake shocks behind the first drop. It is apparent that

the identity of the drop can still be recognized for at least 300 μ sec behind the wave. From the streak photographs it was estimated that the drop is consumed in about 500-600 μ sec for this case in which the equivalence ratio is 0.23 and the velocity is about 3500 ft/sec.

When the drops are closer together than shown in Fig. 6, interactions between the flow fields around each drop and the accompanying shocks become more frequent. This can be seen in Fig. 7 which shows the zone behind the front of detonations travelling at 5200 ft/sec for both 2600 μ and 940 μ sprays. Despite the complicated structure, however, the front is remarkably flat.

B. Development of Detonations

The initiating shock strength in all of the experiments was about Mach 2.5-3.0. Detonations were consistently developed in all three spray sizes when oxygen was used. However, no detonations developed with air as oxidizer.

The effect of drop size on the development time can be seen from Fig. 8, where a plot of the wave velocity as a function of distance from the initiation point is shown. The equivalence ratio beyond 4 ft from the injection point for all of the three sizes used was about 0.25. It is apparent that the smaller the drop size the faster the detonation reaches a nearly steady velocity. It should be pointed out that this effect would have been more pronounced were it possible to have the

same mixture ratios in the first 4 ft. As it was, because of the nature of the spray generator⁷, the mixture ratio in the first 4 ft is leaner for the 290 μ and richer for the 940 μ and the 2600 μ drops. This non-uniform mixture distribution would tend to either delay the detonation development in the 290 μ spray or speed it in the 940 μ and the 2600 μ sprays.

Measurement of the steady velocity was made for mixtures at equivalence ratios ranging from 0.2 to 1.0. The data for the three drop sizes is shown in Fig. 9 and is compared with the calculated theoretical CJ velocity¹. It can be seen that the velocity difference is about 2-10% for the 290 μ and the 940 μ sprays but about 30-35% for the 2600 μ . This difference will be shown, in the next section, to be due to heat transfer and friction losses to the tube walls in the reaction region.

EFFECT OF DROP SIZE ON VELOCITY DIFFERENCE

The reaction region here is assumed to be the region between the front of the wave and the CJ plane. In this region the flow is complicated by drop deformation and breakup, interactions of the two phases, and the chemical reaction due to combustion. However, it is reasonable to assume a one-dimensional flow near the front, which appears to be reasonably planar, as well as after all interactions have

subsided. Such an assumption was made by Ragland⁹ who, after using the conservation equations and taking into account frictional and heat losses, obtained the following equation:

$$\frac{u_s}{u_{so}} = \left\{ 1 + \left[C_D + 2 \left(\gamma_3^2 - 1 \right) C_H \right] \frac{\bar{x}}{(1 + \eta) r_h u_s (u_s - u_2)} \frac{u_2^2}{(u_s - u_2)} \right\}^{-1/2} \quad (1)$$

where u_s is the actual detonation velocity, u_{so} is the ideal CJ velocity, γ_3 is the ratio of specific heats at the Chapman-Jouguet plane, \bar{x} is the reaction length, η is the fuel to oxygen mass ratio, r_h the hydraulic radius of the tube, u_2 is the convective velocity of the oxygen immediately behind the front, and the drag and heat transfer coefficients are defined as

$$C_D = \int_2^3 \bar{\tau} dx / \frac{1}{2} \bar{x} \rho_2 u_2^2 \quad (2)$$

and

$$C_H \equiv \int_2^3 q dx / \rho_2 u_2 \left(h_2 + \frac{u_2^2}{2} - h_w \right) \quad (3)$$

Here, $\bar{\tau}$ is the shear stress at the wall, ρ_2 is the density of oxygen behind the front shock, q the heat transfer rate per unit area of the wall, h_2 and h_w the enthalpy of oxygen behind the shock and at the

wall respectively. Conditions 2 and 3 are immediately behind the front and at the CJ plane respectively.

The heat transfer rate was measured by a thin film gauge so that an estimate of C_H and, if a Reynolds' analogy is assumed, of C_D can be obtained. Estimation of the reaction length, \bar{x} , can be made by assuming that it is controlled by the breakup time. From work¹⁰ done at this laboratory and elsewhere^{11, 12} on the breakup of inert drops by shock waves, the breakup time t_b , can be related to the dynamic pressure of the convective flow and the drop diameter D , as follows:

$$t_b/D = k \rho_\ell^{1/2} \left(\frac{1}{2} \rho_2 u_2^2 \right)^{-1/2} \quad (4)$$

where k is a constant $\cong 5$ and ρ_ℓ is the liquid density. (A similar relation was obtained by Clark¹³ on the breakup of liquid jets.) However, streak photographs of the spray detonation indicated that the time for the breakup of the drop was about double the time calculated by this equation. It is reasoned that since the drop in a detonation is subjected to a varying dynamic pressure, due to the continuously changing conditions behind the front, a better estimate of the actual breakup time in a detonation would be obtained if an average dynamic pressure is used. Since the dynamic pressure in the convective flow behind a CJ plane is about 10% or less than that behind a shock travelling at the same Mach number, for $M > 3$, an average dynamic

pressure equal to half of that in Eq. (4) can be used. Thus Eq. (4) can be modified to read:

$$t_b/D = 2k \left(\frac{\rho_\ell}{\rho_1} \right)^{1/2} \left(\frac{\rho_1}{\rho_2} \right)^{1/2} \left(\frac{1}{u_2} \right) \quad (5)$$

or in terms of the shock velocity:

$$\tau_b \equiv t_b u_s/D = 10 \left(\frac{\rho_\ell}{\rho_1} \right)^{1/2} \left(\frac{\rho_1}{\rho_2} \right)^{1/2} \left(1 - \frac{\rho_1}{\rho_2} \right)^{-1} \quad (6)$$

This equation gives a value of $\tau_b = 162$ for $M = 3$ which decreases to 120 for $M \rightarrow \infty$

With \bar{x} assumed equal to $t_b u_s$ and with $C_D = 2C_H$, Eq. (1) can now be written as

$$\frac{u_s}{u_{so}} = \left\{ 1 + \frac{20D}{(1+\eta) r_h} \gamma^2 C_H \left(\frac{\rho_\ell}{\rho_1} \right)^{1/2} \left(\frac{\rho_2}{\rho_1} \right)^{1/2} \left(1 - \frac{\rho_1}{\rho_2} \right) \right\}^{-1/2} \quad (7)$$

Examples of heat transfer coefficient data are shown in Fig. 10 for detonations in 2600 μ spray. Two different gauges stationed 1 ft apart were used. The velocity corresponds to $M = 3.3$ and it can be seen that a sharp rise in C_H which is followed by a drop, occurs near $\tau_m \equiv t u_s/D \approx 200$. For cases where $M \approx 5$ the rise occurs near $\tau_m \approx 100$. Thus it appears that the point where C_H reaches a

maximum follows the same trend as the nondimensional breakup time. Comparing τ_b and τ_m one finds the difference is not in the same direction for M near 3 as for M near 5. An important difference may be that in the case of $M \approx 5$ the drops are initially subjected to pressures higher than the critical pressure of DECH (25 atm). This is not true for $M \approx 3$. Further investigation is needed to ascertain whether the possible difference is indeed important. For the present we assume that the maximum C_H signals the end of the reaction zone and therefore conclude that the reaction length is controlled by the breakup time.

It should be noted that the product of the last two density ratio terms in Eq. (7) should correspond to u_s . However this product would not differ by much if values corresponding to u_{so} were used. Furthermore, for mixtures leaner than twice stoichiometric an increase in η corresponds to an increase in u_{so} and therefore in the product of the density terms. Thus Eq. (7) can be approximated by

$$\frac{u_s}{u_{so}} = \left\{ 1 + \frac{30D}{r_h} \gamma_3^2 \left(\frac{\rho_l}{\rho_1} \right)^{1/2} C_H \right\}^{-1/2} \quad (8)$$

Using a value of $C_H = 2.5 \times 10^{-3}$ (which is our best up-to-date estimate) and $\gamma_3 = 1.2$, we obtain for our tube ($r_h = 1.04$ cm) for $D = 2600\mu$, 940μ and 290μ , $u_s/u_{so} = 0.76$, 0.90 and 0.96 respectively. These values are in reasonable agreement with the experimental

results shown in Fig. 9. Thus although the structure of the spray detonation is very complicated, it appears that the one-dimensional theory with frictional and heat transfer losses in a reaction zone controlled by the breakup time can offer useful predictions of the detonation velocity.

CONCLUSIONS

The development time of a spray detonation decreases with decreasing drop diameter. For the fully developed wave the velocity is lower than the predicted ideal velocity. The difference is dependent directly on the drop size whose breakup time can be related to the reaction length.

ACKNOWLEDGMENT

The authors are grateful to NASA for supporting this work under Contract NASr 54(07), and wish to thank Messrs. R.C. Stitt, D. Giere and H.D. Radcliff for their assistance with the experiments.

REFERENCES

1. Dabora, E.K., Ragland, K.W., and Nicholls, J.A., *Astronautica Acta*, 12, 9 (1966).
2. Williams, F.A., Progress in Astronautics and Rocketry, Vol. 6, Detonation and Two-Phase Flow (S.S. Penner and F.A. Williams, Ed.), p. 99, Academic Press, 1962.
3. Webber, W.T., Eighth Symposium (International) on Combustion, p. 1129, Williams and Wilkins, 1962.
4. Cramer, F.B., Ninth Symposium (International) on Combustion, p. 482, Academic Press, 1963.
5. Morris, D.H., Wojcicki, S. and Oppenheim, A.K., Development of Detonation in Liquid Fuel Spray with Gaseous Oxidizer—Preliminary Experiments, NASA CR-80098, 1966.
6. Ragland, K.W. and Cullen, R.E., *Rev. Sci. Instr.*, 38, 740, (1967).
7. Dabora, E.K., *Rev. Sci. Instr.*, 38, 502 (1967).
8. Pirroni, J.S. and Stevens, R.R., *Rev. Sci. Instr.*, 38, 382 (1967).
9. Ragland, K.W., The Propagation and Structure of Two Phase Detonations, Ph.D. Thesis, The University of Michigan, 1967.
10. Dabora, E.K., Ragland, K.W., Ranger, A.A., and Nicholls, J.A., Two Phase Detonations and Drop Shattering Studies, NASA CR 72225, 1967.

11. Engel, O.G., J. Research Natl. Bur. Standards, 60, 245 (1958).
12. Nicholson, J.E. and Hill, A.F., Rain Erosion on Spike Protected Supersonic Radomes, Mithras, Inc., Cambridge, Mass. Report MC-61-6-R3, 1965.
13. Clark, B.J., Breakup of a Liquid Jet in a Transverse Flow of Gas, NASA TN D-2424, 1964.

FIGURE CAPTIONS

- Fig. 1. Schematic Diagram of Spray Detonation Apparatus.
- Fig. 2. Examples of Sprays Viewed at the Lower Observation Window
(a) 290μ , (b) 940μ , (c) 2600μ .
- Fig. 3. Schlieren Streak Photograph of Detonation in 290μ Spray
(Run No. 380).
- Fig. 4. Combined Shadow and Direct Luminosity Streak Photograph
of Detonation in 940μ Spray (Run No. 130).
- Fig. 5. Combined Shadow and Direct Luminosity Streak Photograph
of the Detonation over a Single Stream of 2600μ Drops
(Run No. 278).
- Fig. 6. Spark Source ($.2\ \mu\text{sec}$ exposure) Photograph of the Detonation
of Single Stream of 2600μ Drops Showing Details of the
Phenomenon (Runs No. 452, 435, 436).
- Fig. 7. Spark Source Photograph of the Detonation of (a) 4 Streams
of 2600μ Drops (Run No. 465) and (b) 940μ Sprays (Run No.
445).
- Fig. 8. Development of Detonation Wave.
- Fig. 9. Comparison of Experimental Detonation Velocity with the
Ideal CJ Velocity.
- Fig. 10. Examples of Calculated Heat Transfer Coefficient from
Thin Film Heat Gauge Measurements.

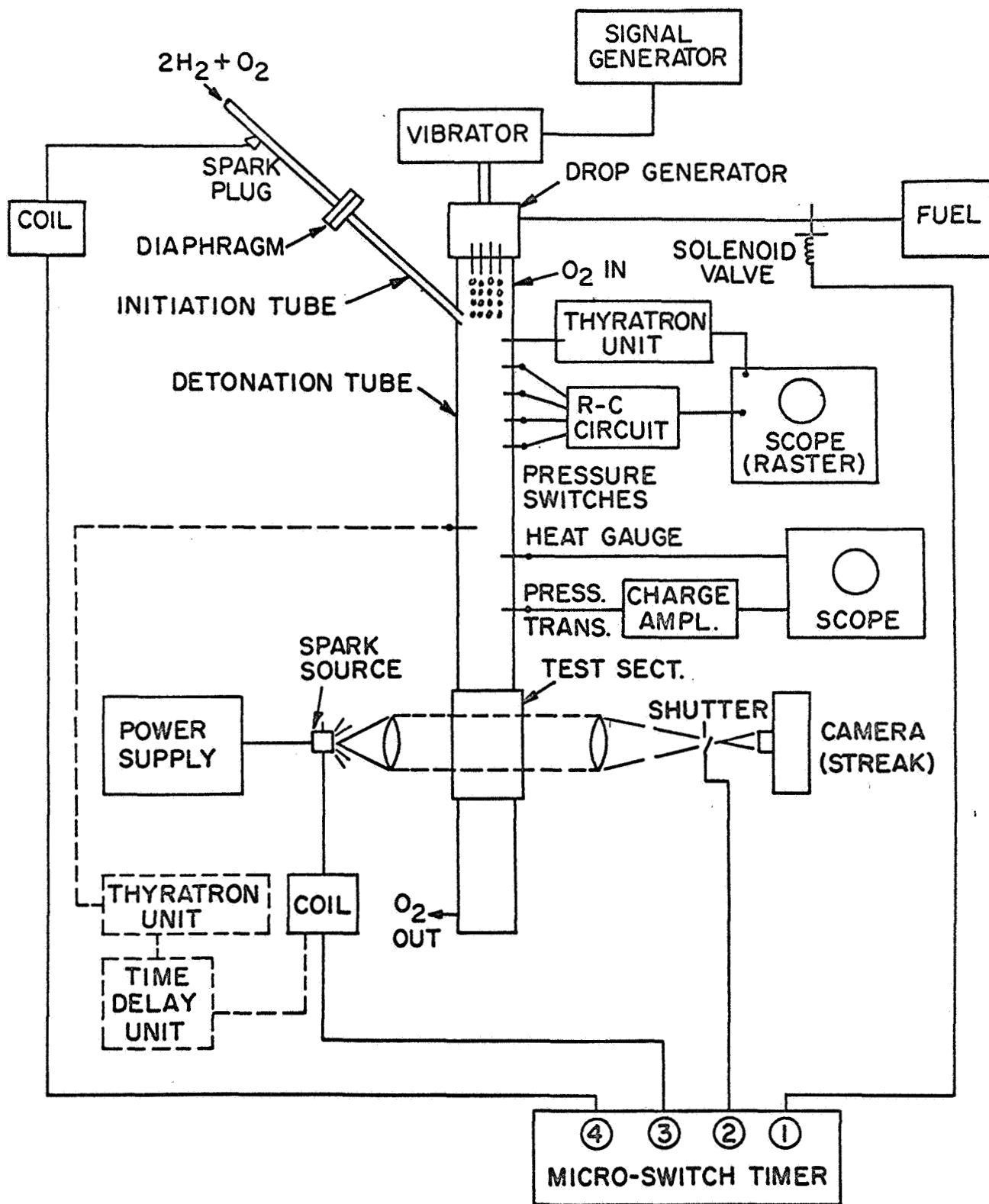


Fig 1

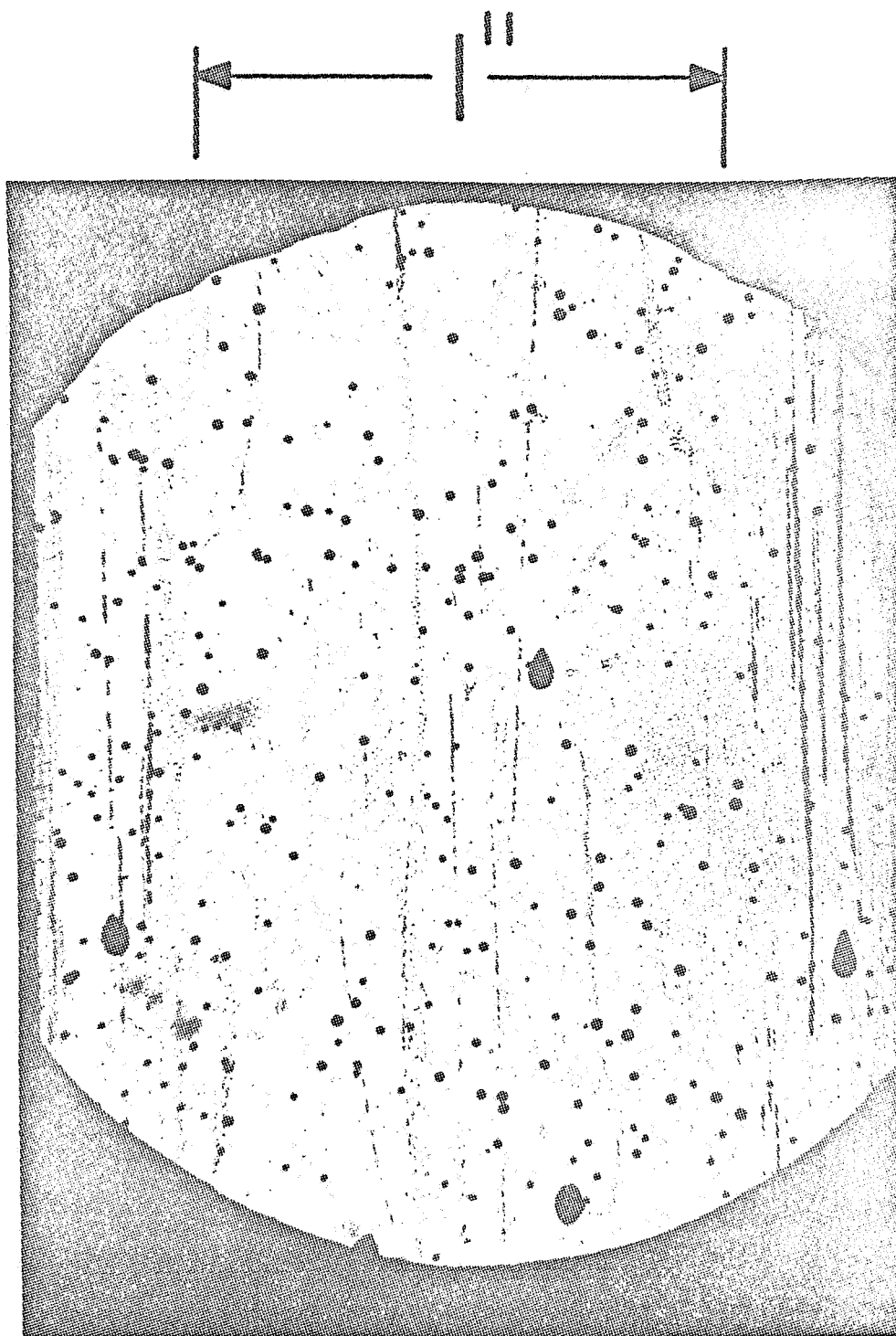


Fig 2a

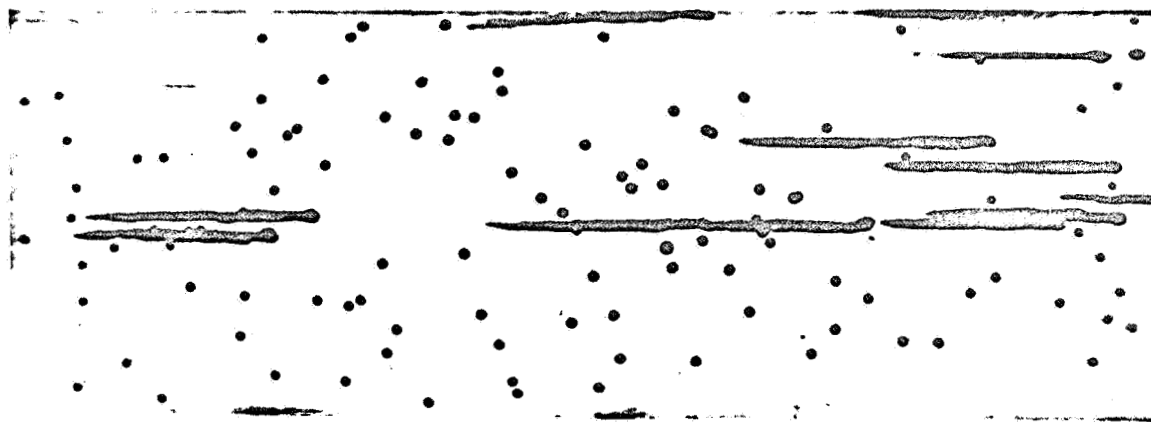
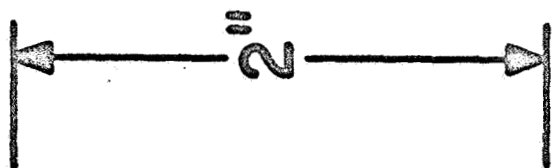
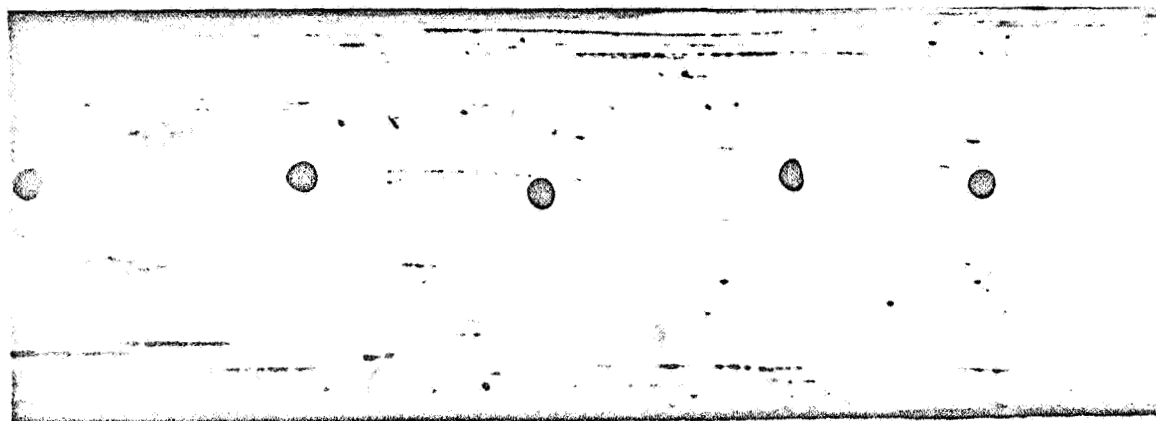


Fig 2 b & c

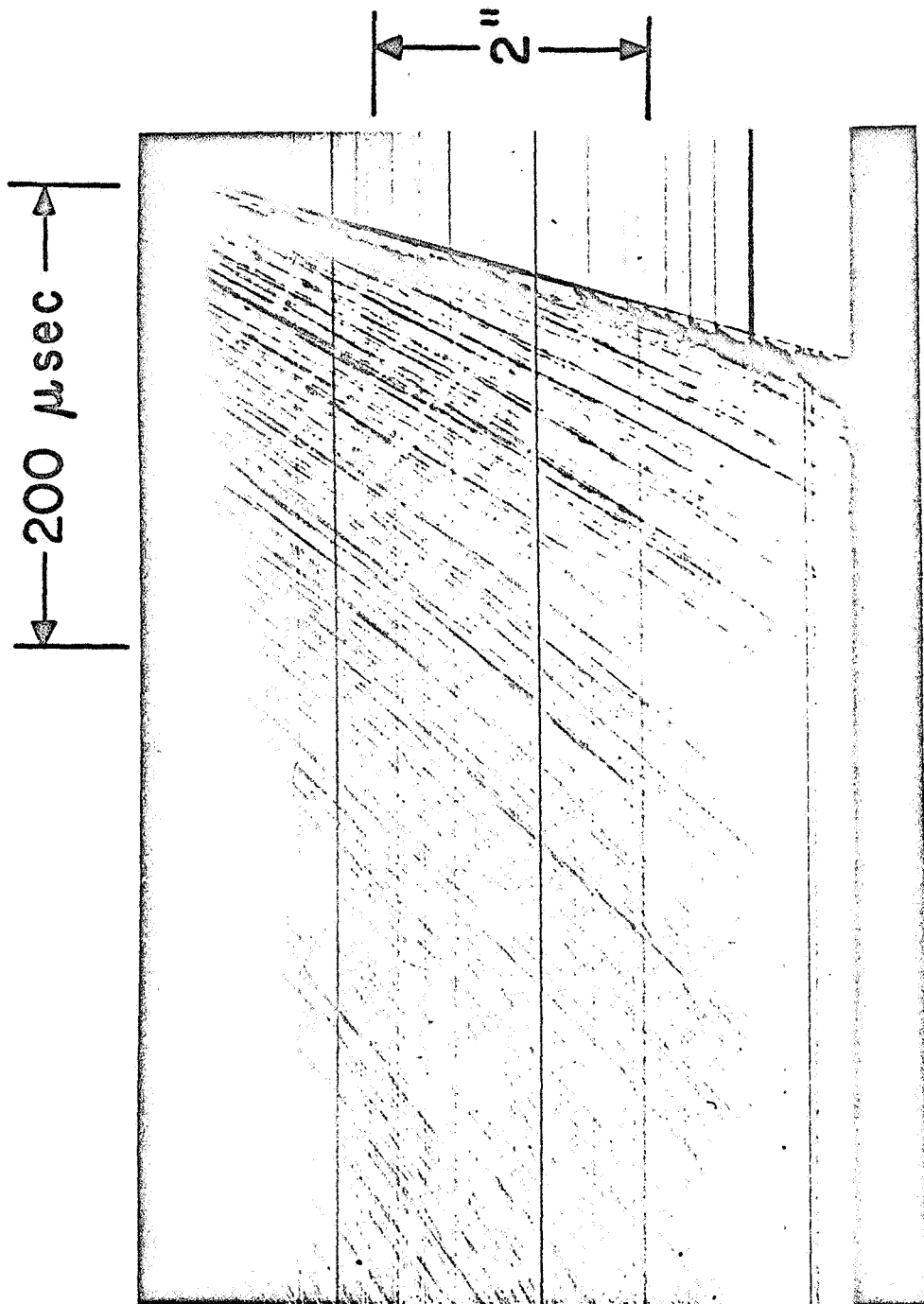


Fig 3

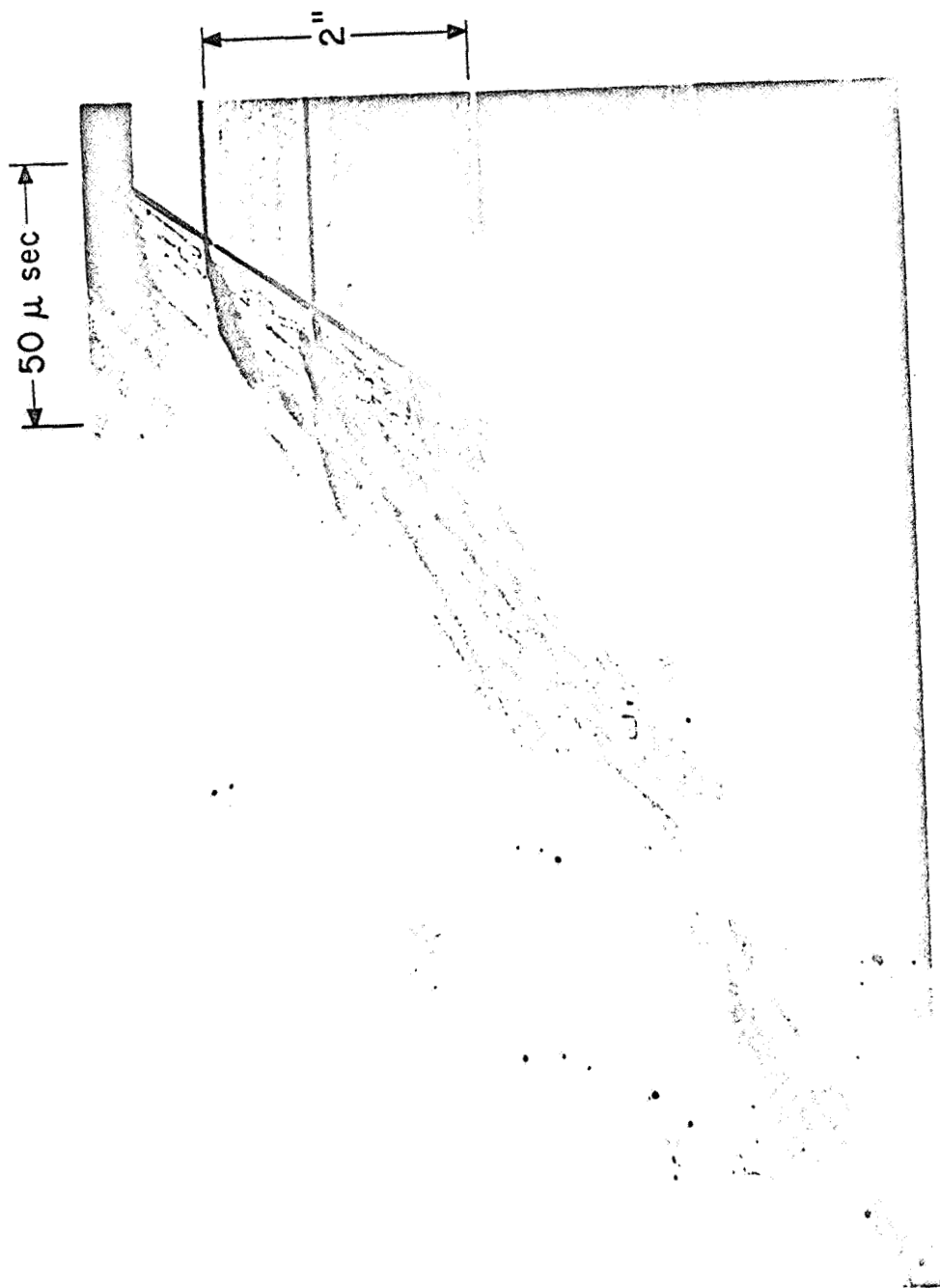


Fig 4

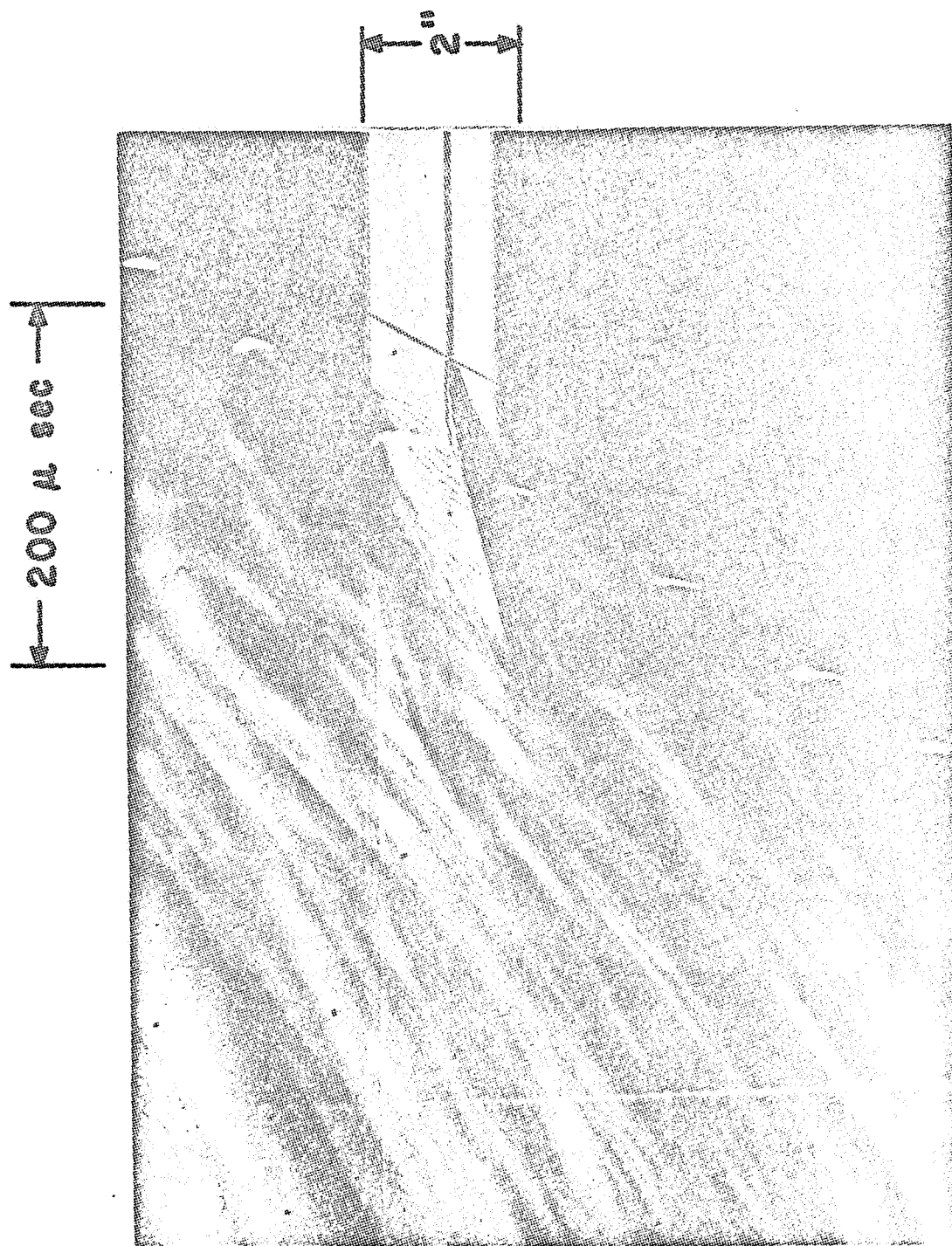


Fig 5

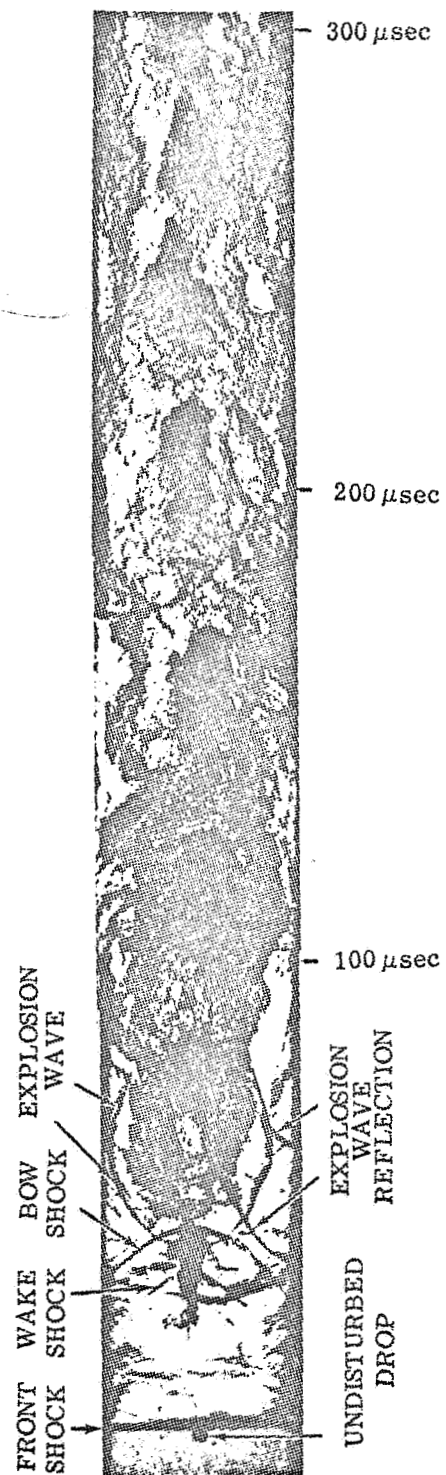


Fig 6

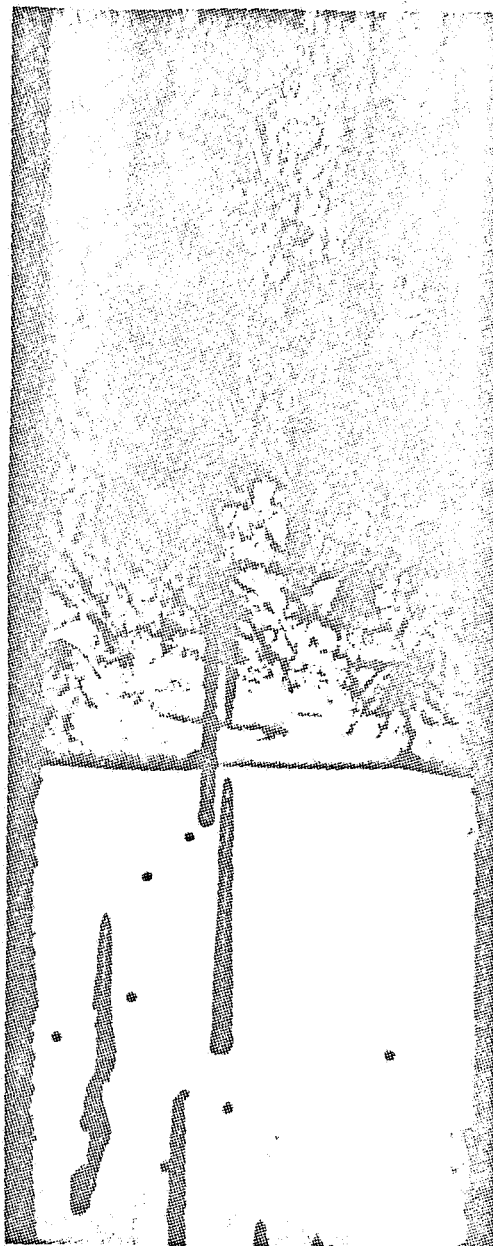
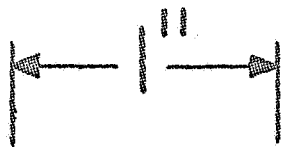
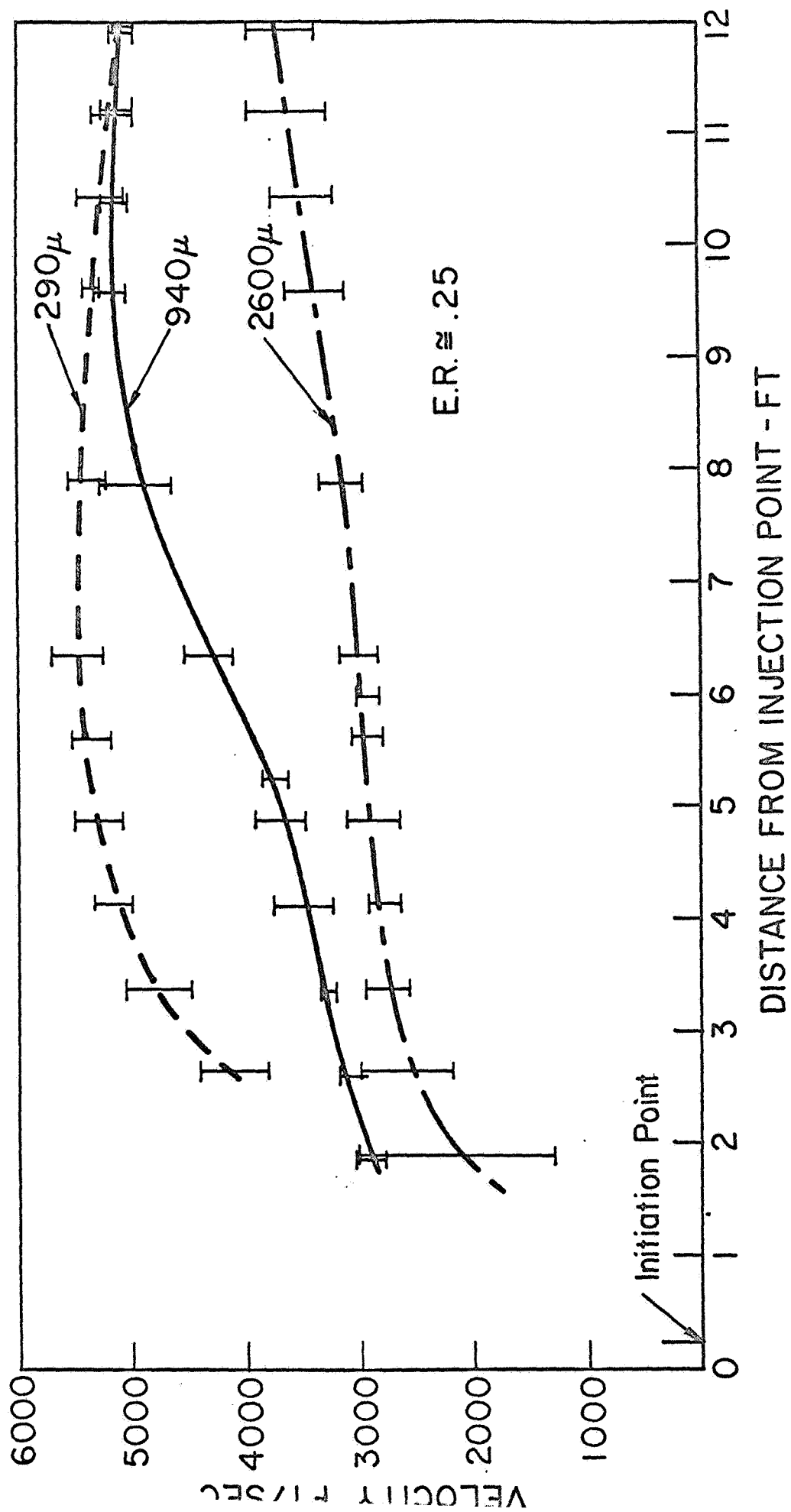
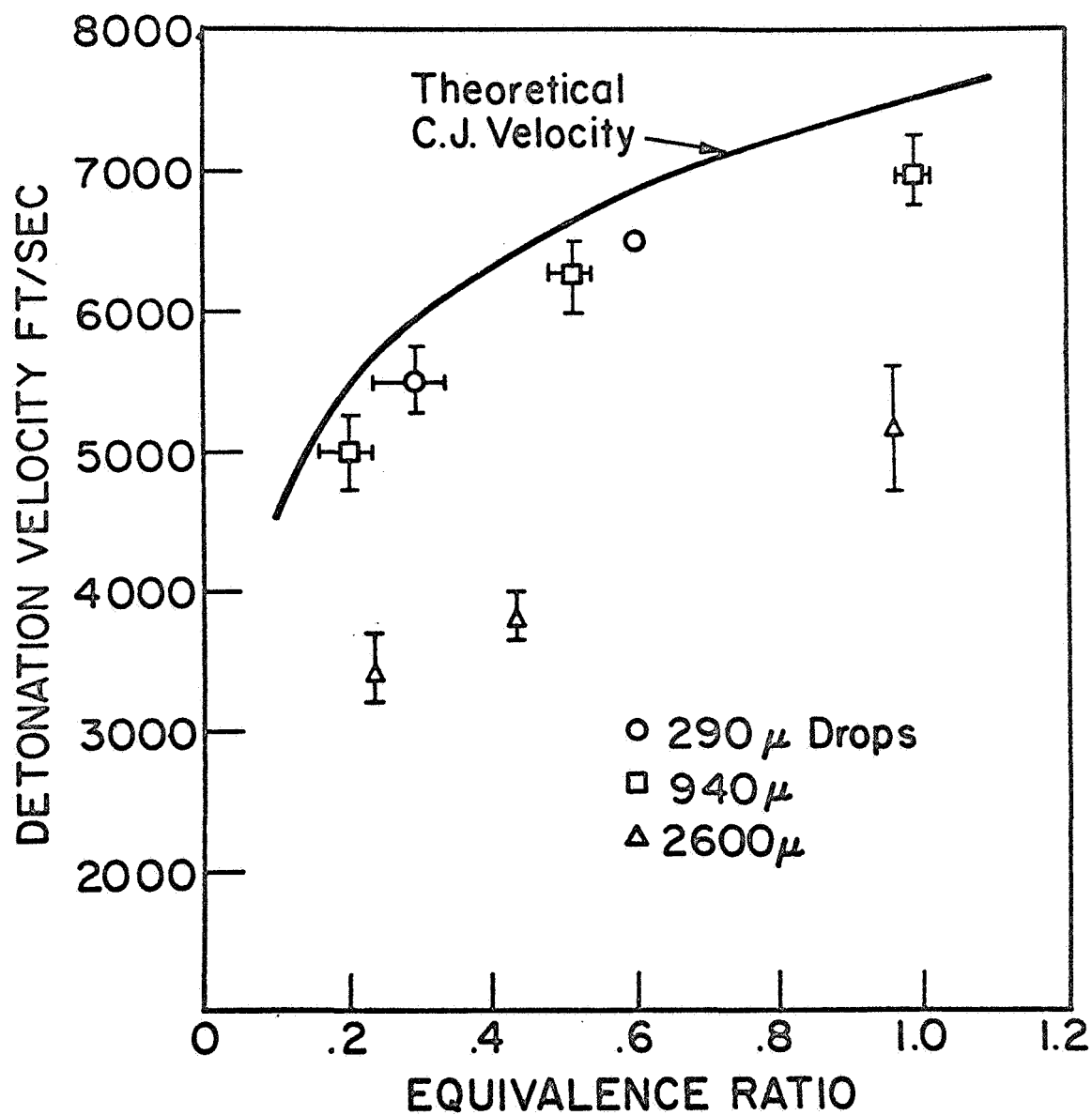
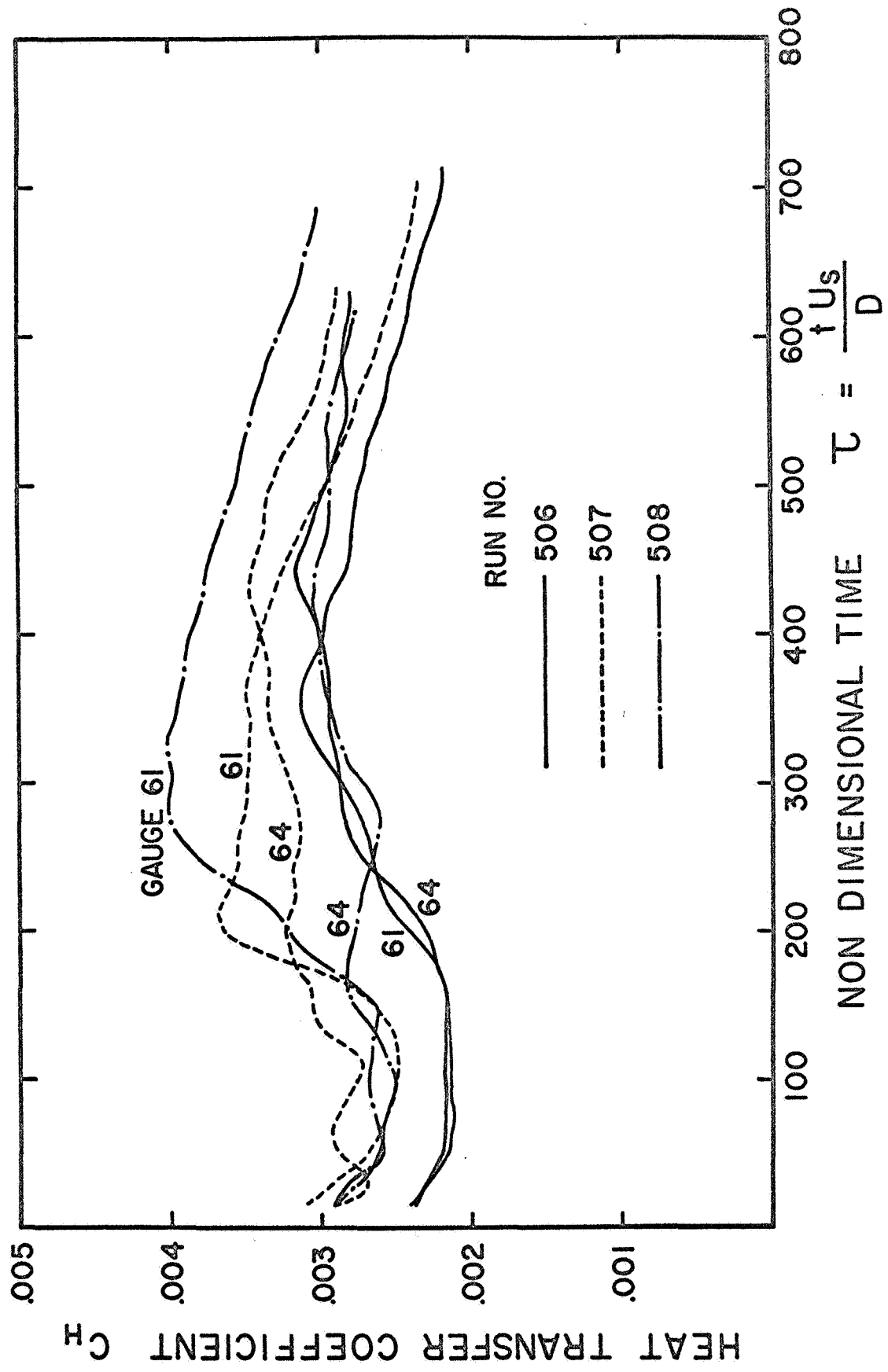


Fig 7





759



25/10